

CFD Modeling of Reactive Pollutants in an Urban Street Canyon using Different Chemical Mechanisms

B Sanchez^{a,b,*}, JL Santiago^a, A Martilli^a, M Palacios^a, F Kirchner^c

^a*Center for Energy, Environment and Technology (CIEMAT), Madrid, Spain*

^b*Ingeniería y Economía del Transporte (INECO). Avda. Partenón 4-6, 28042 Madrid, Spain*

^c*GAIASENS Technologies. Sarl, Switzerland*

1. Introduction

An accurate understanding of urban air quality requires considering a coupled behavior between dispersion of reactive pollutants and atmospheric dynamics. Currently, urban air pollution is mostly dominated by traffic emissions. Only fast chemical reactions have influence on street pollutant concentration due to the proximity between sources and receptors. Therefore, some low reactive traffic-related pollutants like CO can be considered as practically inert species at microscale. However, nitrogen oxide (NO) and nitrogen dioxide (NO₂) reacts extremely fast (time scales of the order of tens of seconds), and the fact that Volatile Organic Compounds (VOCs) are also involved in this complex chain of reactions. To properly account for VOCs, a complex chemical mechanism is needed with several chemical reactions that require a significant amount of CPU time. Including the vast number of chemical species and reactions that occur in the urban atmosphere is not possible, and it is necessary to choose the most suitable mechanism for each scenario in terms of accuracy and CPU time.

The aim of this work is to model the chemical and dynamic coupling focusing on the NO and NO₂ dispersion under different chemical approaches in simple urban configurations using a CFD-RANS model. In order to quantify the errors linked with the use of a simplified chemistry, three types of simulations are performed: a) NO and NO₂ as passive tracer (no-reactive), b) NO_x – O₃ photostationary state (PSS), and c) a more complex chemical mechanism (CCM) based on the RACM ('Regional Atmospheric Chemistry Mechanism') in the case of an urban atmosphere and developed to reduce the chemical system to 23 species and 25 reactions using CHEMATA software (Kirchner, 2005). Furthermore, the effect of using a simple chemical mechanism instead of a complex chemical scheme (with two VOCs-to-NO_x emission ratio) is studied. For that, the influence of different atmospheric parameters (zenith angle and wind speed) on NO and NO₂ concentration is evaluated. In this work, some criteria about what type of chemical mechanism is necessary to reproduce NO and NO₂ concentration within streets are provided for different scenarios.

2. Model description

2.1. CFD Model

The Computational Fluid Dynamic (CFD) model used for this study is based on the Reynolds-averaged Navier-Stokes equations (RANS) with a k- ϵ turbulent model. In addition, a transport equation for chemical species is solved. The effect on NO and NO₂ concentrations (hereafter, referred as [NO] and [NO₂] respectively) due to chemical processes are compared with NO and NO₂ simulated as non-reactive pollutants.

*Corresponding author.

Email addresses: beatriz.sanchez@externos.ciemat.es (B Sanchez), jl.santiago@ciemat.es (JL Santiago), alberto.martilli@ciemat.es (A Martilli), magdalena.palacios@ciemat.es (M Palacios), frank.kirchner@gmx.ch (F Kirchner)

Including chemical reactions, the first mechanism considered is the photostationary state (PSS) that is defined by a three-reaction system.



Where M represents a molecule that absorbs excess energy and thereby stabilizes O_3 molecule formed (Seinfeld and Pandis, 1998). The photolysis rate (J_{NO_2}) and reaction rate constant (k) are dependent on zenith angle (θ) and temperature respectively. On the other hand, a complex chemical mechanism (CCM) is considered. Due to limitation of CPU time, the RACM have been reduced to reproduce the urban atmosphere of the Madrid City (Spain). The reduced CCM consists of 25 reactions for 23 chemical species and has been developed using CHEMATA software (Junier et al., 2005; Kirchner, 2005). The chemical term is defined as formation and depletion of a compound in the chemical reactions. It is introduced as a production rate in the transport equation for each chemical specie in the CFD model. Emission term is also added (S_{C_i}). Hence the transport equations are given by,

$$\frac{\partial C_i}{\partial t} + U_i \frac{\partial C_i}{\partial x_j} = D \frac{\partial^2 C_i}{\partial x_j \partial x_j} + \frac{\partial}{\partial x_j} \left(K_c \frac{\partial C_i}{\partial x_j} \right) + \left[\frac{\partial C_i}{\partial t} \right]_{Chem} + S_{C_i} \quad (4)$$

Where C_i is the concentration of the i th specie and D and K_c are molecular diffusivity and eddy diffusivity of pollutants, respectively.

2.2. Simulation Set up

Fig. 1 shows the two different computational domains used: a single street-canyon (2D-geometry) and a staggered array of cubes (3D geometry). The street-canyon and staggered array of cubes domain sizes are 24x40x64 m and 64x64x64m in x, y and z directions respectively. The grid resolution is 1m in all directions. In both geometries, the street canyon aspect ratio defined as the ratio of building height (H) to the street width (W) is unity. The three-dimensional array of cubes is represented by staggered cubes with buildings width (L)(a packing density, $\lambda = 0.25$). And the domain top is located at 4H.

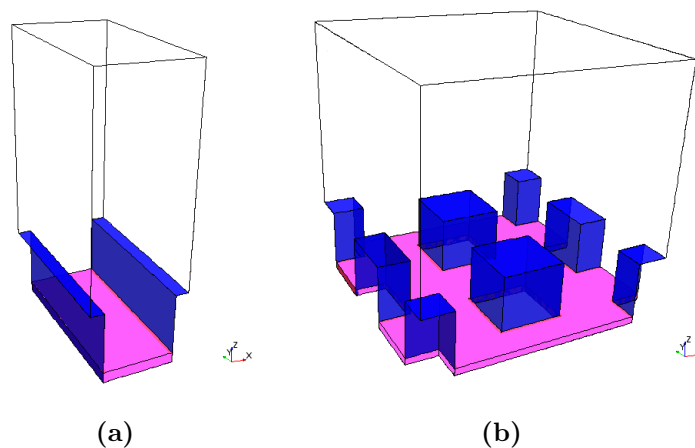


Figure 1: Illustration of the computational domains:(a) 2D geometry (Street Canyon) with H=16m and W=16m and(b) 3D geometry (Staggered array of cubes) with H, W and L equal to 16 m.

Symmetry boundary conditions are assumed in the spanwise direction (y-direction) and periodic conditions are imposed in the streamwise direction in order to simulate an infinite number of streets. The flow is driven in x-direction by pressure gradient equal to $\rho u_\tau^2 / 4H$, where u_τ is the friction velocity. For this study, two friction velocities ($u_\tau = 0.45$ and $u_\tau = 0.45/2$) are used. At the top, symmetry conditions are established that enforce parallel flow and zero normal derivatives for all other variables are imposed (Santiago and Martilli, 2010).

Emission sources are located at ground level in both domains (Fig. 1). Traffic emissions are simulated considering a NO_x emission of 0.5 g km^{-1} per vehicle and volumetric ratio of NO and NO_2 emission is 10:1

(Baker et al., 2004; Baik et al., 2007). Thus NO and NO₂ emissions are fixed with rates of 112 $\mu\text{g m}^{-1} \text{s}^{-1}$ and 17 $\mu\text{g m}^{-1} \text{s}^{-1}$ respectively. And it is equivalent to 930 vehicles per hour representing medium traffic. In addition, with CCM, VOCs emissions are necessarily considered. The ratio VOCs-to-NO_x emitted by vehicles is dependent on several factors such as kind of vehicle or traffic flow speed. For that two different VOCs-to- NO_x emission ratios (1/5 and 1/2) are simulated. Some VOCs are joined in specific chemical groups. The VOCs emitted species considered in the complex chemical scheme are OLE, ARO, ALK, ALD and HCHO, and their volumetric proportions are 28.6%, 23.1%, 38.6%, 4.0% and 5.6%.

Due to periodic and symmetry conditions along x-direction and y-direction respectively, the concentrations at the top play an important role considering chemical reactions. For that reason, the initial concentrations of reactive species are also imposed at top of the domain. The value of NO, NO₂, CO and SO₂ concentration is fixed at 16, 35, 200 and 2 ppb in all simulations. However, O₃ and VOCs concentrations change according to the simulated scenario in order to reach a stationary state. VOCs concentrations are established on the same proportion of VOCs-to-NO_x emission ratios. The corresponding VOCs concentration at the top in VOCs/NO_x=1/2 and VOCs/NO_x=1/5 emission scenario are 25.5 and 10.2 ppb respectively. And the O₃ concentration (hereafter, referred as [O₃]) imposed at the top is computed using the photostationary equilibrium given by,

$$[\text{O}_3] = \frac{J_{\text{NO}_2}[\text{NO}_2]}{k[\text{NO}]} \quad (5)$$

With k, [NO] and [NO₂] constant, the photolysis rate J_{NO_2} is calculated as a function of zenith angle ($J_{\text{NO}_2} = A \exp(B/\cos(\theta))$). Therefore, [O₃] is 10.6 and 39.8 ppb as a result of two different zenith angle used 78° and 46° respectively.

In order to evaluate the results, the normalized concentration of the pollutants is computed using a scale length (l), a reference velocity (u_τ) and source emission rate (Q) following,

$$C_{\text{norm}} = \frac{C u_\tau l^2}{Q} \quad (6)$$

Hereafter, the NO and NO₂ normalized concentration are referred as [NO]_N and [NO₂]_N.

3. Evaluation of atmospheric parameters in [NO] and [NO₂] in 2D and 3D geometry

The CFD model is used to simulate turbulent flow and dispersion of reactive species in a 2D street canyon and a 3D staggered array of cubes. The interaction between the atmosphere and buildings configuration induces complex flow patterns within the urban canopy, and thus changes on pollutant dispersion. Therefore, the time of each compound inside the street have influence on the chemical transformations, and then in the resulting concentrations within the street. The differences of flow patterns in both configurations can be observed in Fig. 2.

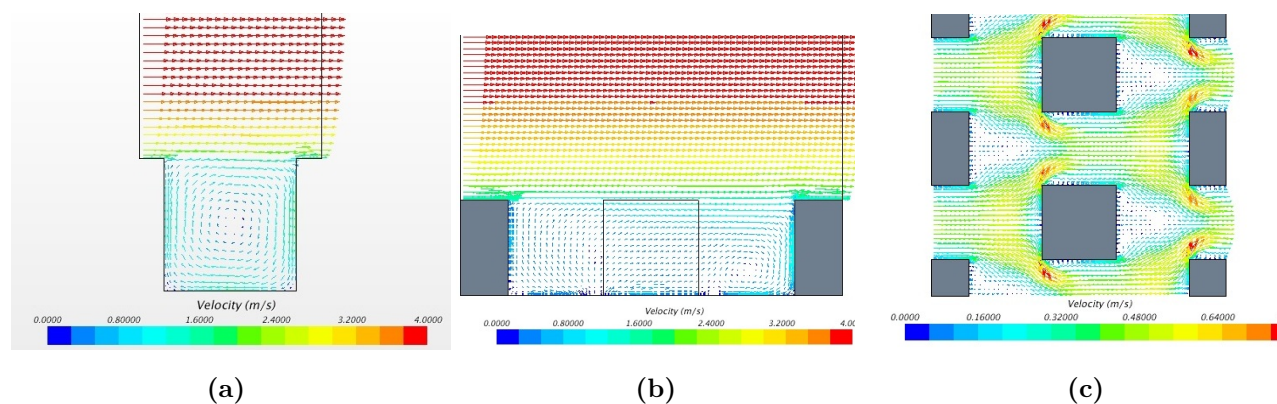


Figure 2: Mean flow field in (a) street canyon along the x-direction and in staggered array of cubes at (b) $y/H=2$ and (c) $z/H=0.125$

3.1. Zenith angle influence on reactive pollutants

Photolysis rates are defined by solar position using zenith angle. Consequently, the amount of O_3 available is dependent on equilibrium relation (eq. 5). For two representative cases of winter ($\theta = 78^\circ$) and summer ($\theta = 46^\circ$) at 0900UTC, the NO and NO_2 are simulated using PSS and CCM with two different VOCs-to- NO_x emission ratios and compared with NO and NO_2 considered as non-reactive species. Fig 3 illustrates vertical profiles of horizontal spatial average of $[NO]_N$ and $[NO_2]_N$ obtained for the different chemical mechanisms with a $\theta = 78^\circ$ ($O_3=10.6$ ppb at top) and $\theta = 46^\circ$ ($O_3=39.8$ ppb at top) in 2D and 3D configurations.

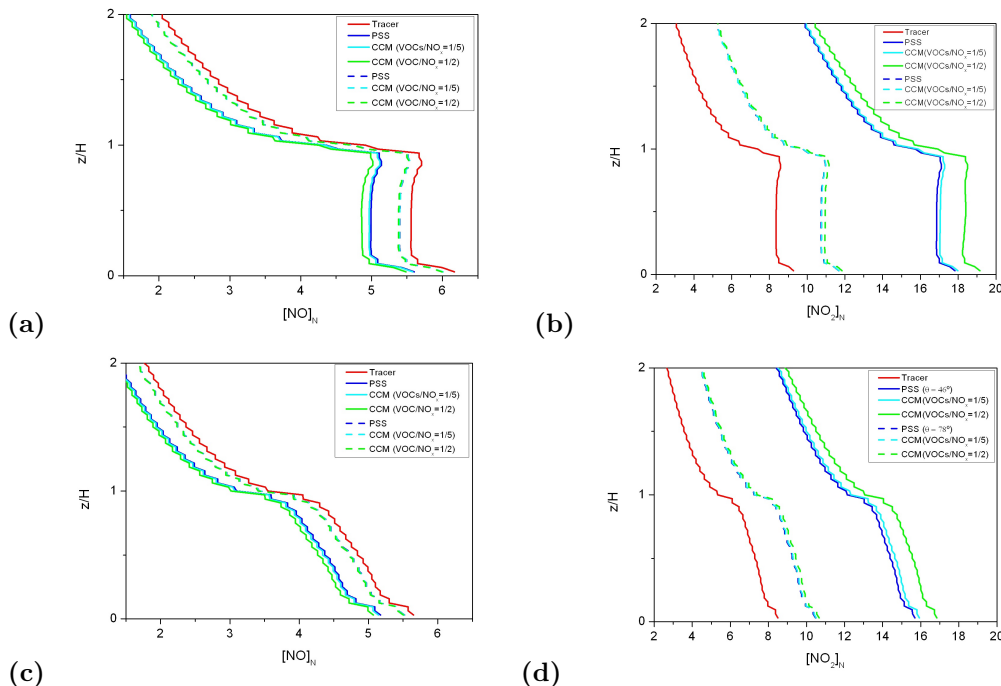


Figure 3: Vertical profiles of horizontal spatial average of $[NO]_N$ and $[NO_2]_N$ obtained for the different chemical mechanisms with a $\theta = 78^\circ$ (dotted line) and $\theta = 46^\circ$ (solid line) in 2D (a,b) and 3D (c,d) geometries.

The importance of using a complex chemical scheme instead of a simplified chemical mechanism in the different geometries is evaluated comparing the $[NO]_N$ and $[NO_2]_N$ with the normalized concentration of passive tracers. In the cases with $\theta = 78^\circ$ (lower O_3 at top), the difference between chemical mechanisms is insignificant. The deviation of $[NO]_N$ in the three chemical scenarios in comparison to tracer is around 3% in all vertical profiles for both geometrical configurations. Likewise for vertical $[NO_2]_N$ this variation is around 30% because the concentration of NO is much higher than NO_2 (emissions of NO are ten times the emissions of NO_2). In all vertical profiles, the average value of the differences between PSS and CCM($VOCs/NO_x=1/5$) and CCM($VOCs/NO_x=1/2$) for $[NO]$ and $[NO_2]$ are approximately 0.2 and 2 ppb respectively. However, when $[O_3]$ is higher ($\theta = 46^\circ$), the importance of the chemical mechanism used increases. The variation of $[NO]_N$ and $[NO_2]_N$ depending on chemical scheme used is observed in the vertical profiles in both domains (Fig. 3). In order to quantify these differences, the average value of concentration within the canopy is compared. The deviation of $[NO]_N$ respect to tracer is around 10.1, 10.5 and 12.3% with PSS, CCM($VOCs/NO_x=1/5$) and CCM($VOCs/NO_x=1/2$), respectively for 2D geometry. In contrast, $[NO]_N$ for all mechanisms are shifted around 9% from $[NO]_N$ no-reactive in the 3D-geometry. Focusing on $[NO_2]_N$, the influence of chemical mechanism is more remarkable in percentage respect to non-reactive pollutant concentration. For PSS, CCM($VOCs/NO_x=1/5$) and CCM($VOCs/NO_x=1/2$), $[NO_2]_N$ increases more than 100%, with differences until 10 ppb in the 2D configuration and 7 ppb in the staggered array of cubes. Therefore, the $[O_3]$ at the top modifies the influence of the chemical mechanism within the street.

The influence of VOCs-to- NO_x emission ratio on $[NO]_N$ and $[NO_2]_N$ comparing the CCM and PSS is analyzed with respect to normalized concentration of passive tracer ($[NO(P)]_N$ and $[NO_2(P)]_N$). The $[NO]_N$ and $[NO_2]_N$ at 3m is studied in order to determine how concentration close to ground is deviated depending on chemical mechanism and emission ratio in 2D and 3D configurations (Fig. 4). Overall, comparing $[NO]_N/[NO(P)]_N$ and $[NO_2]_N/[NO_2(P)]_N$ for both configurations, the differences are 1% and 4% lower for 3D

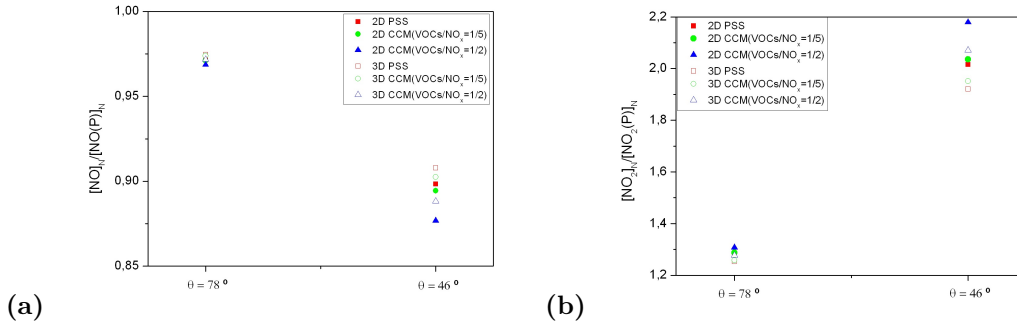


Figure 4: Spatial average of $[NO]$ and $[NO_2]_N$ at 3m for PSS and CCM with VOCs-to-NO_x equal to 1/5 and 1/2 in 2D and 3D geometrical configuration for

with respect to 2D geometry. With lower $[O_3]$, the effect of VOCs emissions on $[NO]_N$ and $[NO_2]_N$ is negligible in both geometries. Hence the photostationary state or complex chemical mechanism can be used to reproduce the NO and NO₂ dispersion. However, in the higher O_3 case, the differences between chemical schemes increase within the canyon. For instance, in 2D geometry, $[NO]_N/[NO(P)]_N$ is 0.87, 0.89 and 0.90 whereas $[NO_2]_N/[NO_2(P)]_N$ varies from 2.07, 1.95 and 1.92 for CCM(VOCs/NO_x=1/2), CCM(VOCs/NO_x=1/5) and PSS respectively. Hence with higher $[O_3]$, the VOCs-to-NO_x emission ratio has influence on $[NO]$ and $[NO_2]$. A high $[O_3]$, strong NO and VOCs traffic emissions increase considerably the NO₂ production inside the street. Therefore, in order to simulate $[NO]$ and $[NO_2]$ in an urban area with high VOCs-to-NO_x traffic emissions and high $[O_3]$, a complex chemical mechanism is required.

3.2. Wind speed influence on reactive pollutants

The concentration of a non-reactive pollutant is inversely proportional to wind speed. However, the non linearity of chemical reactions introduces changes in the concentration behavior. In order to analyze the effect produced by wind speed on NO and NO₂ concentration, two scenarios with different velocities (Ut045: $u_\tau=0.45\text{ m/s}$ and Ut0225: $u_\tau = 0.45/2\text{ m/s}$) are simulated (Fig. 5).

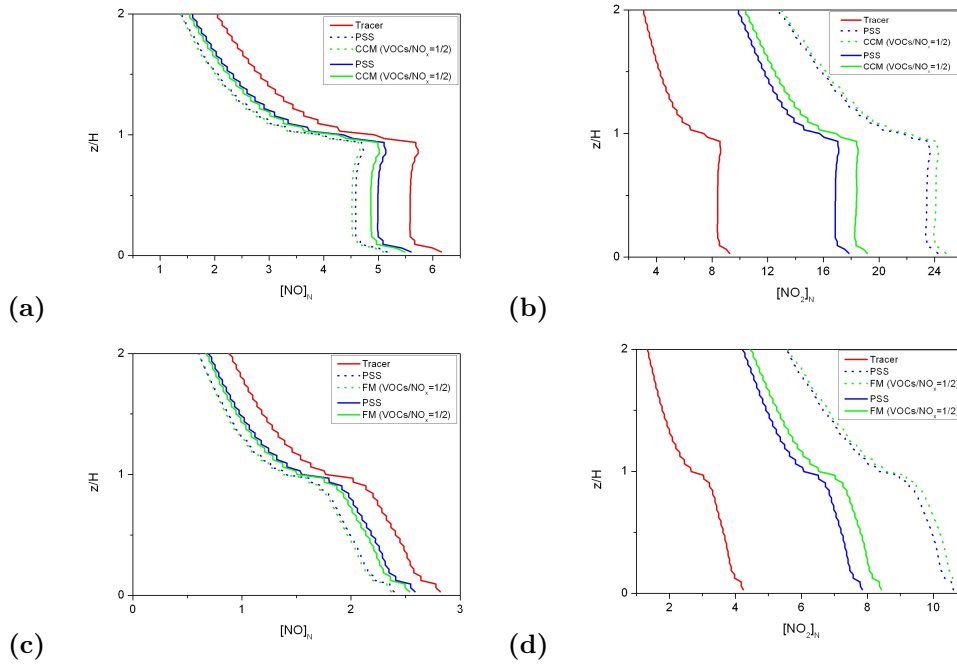


Figure 5: Vertical profiles of horizontal spatial average of $[NO]_N$ and $[NO_2]_N$ obtained for the different chemical mechanisms with a $u_\tau=0.45\text{m/s}$ (dotted line) and $u_\tau=0.45/2\text{ m/s}$ (solid line) in 2D (a,b) and 3D (c,d) geometries.

In these simulations, zenith angle is held constant at 45° because as discussed in the previous section, for this angle the influence of chemical processes is higher than for $\theta=78^\circ$. The strong accumulation of NO_x within the street contributes to consume quickly $[\text{O}_3]$ and intensify the NO_2 formation and NO depletion. The influence of chemistry respect to non-reactive pollutant is lower for Ut0225 than for Ut045 in terms of normalized concentration. In average below the canopy, $[\text{NO}]_N$ is shifted around 18% and 10% respect to tracer for Ut0225 and Ut045, respectively. Whereas $[\text{NO}_2]_N$ is increased a factor 2 and 2.7 for Ut045 and Ut0225. Note that while the normalized concentration is proportional to concentration and inversely proportional to wind speed, the effect of chemical reactions is not proportional to wind speed. In addition, analyzing the effect of VOCs emissions on $[\text{NO}]$ and $[\text{NO}_2]$, the higher differences between chemical mechanisms are produced for Ut0225 scenario. The concentration differences linking to chemical mechanism used to describe NO and NO_2 dispersion is slightly dependent on wind speed within the street.

4. Conclusions

The main conclusion is that errors induced by the use of the simple photochemistry state are larger when the VOCs-to- NO_x emission ratio increases in presence of high $[\text{O}_3]$. For this case, considering VOCs chemical reactions, lower $[\text{NO}]$ and higher $[\text{NO}_2]$ are obtained in comparison with steady state photochemistry. In contrast, with lower $[\text{O}_3]$ at the top of the domain, $[\text{NO}]$ and $[\text{NO}_2]$ can be simulated by photostationary state or complex chemical mechanisms due to the differences between mechanisms are negligible. Additionally, the influence of wind speed is evaluated to establish a relation with $[\text{NO}]$ and $[\text{NO}_2]$. The non linearity of chemistry induces that $[\text{NO}]$ and $[\text{NO}_2]$ are not inversely proportional with respect to wind speed, a different behavior in comparison with a non-reactive pollutant. Overall, the influence of a complex chemical mechanism is slightly smaller in 3D than 2D geometry since major ventilation is produced within the street. Hence smaller residence time of the pollutant in the canopy implies less time to react. However, since high VOCs-to- NO_x emissions under urban conditions are common, the $[\text{NO}]$ and $[\text{NO}_2]$ are accurately reproduced using a complex chemical mechanism.

Acknowledgements

This work is co-funded by INECO and European Union within the framework of European Project LIFE MINOX-STREET (LIFE12 ENV/ES/000280).

References

- Baik, J.-J., Kang, Y.-S., Kim, J.-J., 2007. Modeling reactive pollutant dispersion in an urban street canyon. *Atmospheric Environment* 41 (5), 934–949.
- Baker, J., Walker, H. L., Cai, X., 2004. A study of the dispersion and transport of reactive pollutants in and above street canyons—a large eddy simulation. *Atmospheric Environment* 38 (39), 6883–6892.
- Junier, M., Kirchner, F., Clappier, A., van den Bergh, H., 2005. The chemical mechanism generation programme chemata—part 2: Comparison of four chemical mechanisms for mesoscale calculation of atmospheric pollution. *Atmospheric Environment* 39 (6), 1161–1171.
- Kirchner, F., 2005. The chemical mechanism generation programme chemata—part 1: The programme and first applications. *Atmospheric Environment* 39 (6), 1143–1159.
- Santiago, J., Martilli, A., 2010. A dynamic urban canopy parameterization for mesoscale models based on computational fluid dynamics reynolds-averaged navier–stokes microscale simulations. *Boundary-layer meteorology* 137 (3), 417–439.
- Seinfeld, J. H., Pandis, S. N., 1998. *Atmospheric chemistry and physics: from air pollution to climate change*. John Wiley & Sons.